C. R. Palevol 18 (2019) 1073–1082

Contents lists available at ScienceDirect

Comptes Rendus Palevol

www.sciencedirect.com

Human Palaeontology and Prehistory (Palaeoanthropology)/Paléontologie humaine et préhistoire (Palaeoanthropologie)

Inner structural organization of the mandibular corpus in the late Early Pleistocene human specimens Tighenif 1 and Tighenif 2

Organisation structurale interne du corps mandibulaire chez les spécimens humains Tighenif 1 et Tighenif 2 du Pléistocène inférieur final

Lisa Genochio[a,b], Arnaud Mazurier[c], Jean Dumoncel[a], Charlotte E.G. Theye[d], Clément Zanolli[e,*]

[a] *UMR 5288 CNRS, Université Toulouse-3-Paul-Sabatier, 31062 Toulouse, France*
[b] *Department of Archaeology and Hull York Medical School, University of York, York, UK*
[c] *Institut IC2MP 7285 CNRS, Université de Poitiers, 86022 Poitiers, France*
[d] *Department of Anatomy, University of Pretoria, Pretoria, South Africa*
[e] *UMR 5199 CNRS, Université de Bordeaux, 33615 Pessac, France*

ARTICLE INFO

Article history:
Received 10 February 2019
Accepted after revision 26 September 2019
Available online 29 October 2019

Handled by Roberto Macchiarelli

Keywords:
Mandibular cortical bone thickness
Homo
Late early Pleistocene
Tighenif

ABSTRACT

The present study investigates the inner structural organization of the two mandible specimens Tighenif 1 and Tighenif 2 from the late early Pleistocene site of Tighenif, Algeria. Using (micro)tomographic scans, we built a new protocol to investigate the cortical bone topography at the post-canine level. We selected two cross-sectional slices placed between the P3/P4 and M1/M2 on the right and left sides and assessed the cortical bone thickness topography (CBT) on each slice. Our analyses demonstrate that the mandibles from Tighenif exhibit higher CBT and a different topographic distribution pattern at the molar level than in modern humans, resulting in a proportionally more robust inner structure, while a similar signal is observed between the fossil and extant specimens at the premolar level. Further studies need to be done in order to determine if this feature is related to functional constraints during mastication or paramasticatory activities; or if it is related to any independent evolutionary process.

Mots clés :
Épaisseur de l'os cortical mandibulaire
Homo
Pléistocène inférieur final
Tighenif

RÉSUMÉ

Cette étude examine l'organisation structurale interne des deux spécimens mandibulaires Tighenif 1 et Tighenif 2 du site du début du Pléistocène inférieur final de Tighenif, en Algérie. En utilisant des scans (micro)tomographiques, nous avons construit un nouveau protocole, afin d'étudier la topographie de l'os cortical au niveau des dents jugales. Deux coupes transversales ont été sélectionnées et placées entre les P3/P4 et M1/M2 gauches et droites afin d'y évaluer l'épaisseur de l'os cortical (CBT). Nos résultats montrent que les deux fossiles de Tighenif présentent une épaisseur d'os cortical plus élevée et une distribution de l'os cortical différente au niveau des molaires par rapport aux humains modernes, se traduisant

* Corresponding author.
E-mail address: clement.zanolli@gmail.com (C. Zanolli).

https://doi.org/10.1016/j.crpv.2019.09.002

par une structure interne proportionnellement plus robuste, tandis qu'un signal similaire est observé entre les spécimens fossiles et actuels au niveau des prémolaires. Cependant, des études complémentaires seront nécessaires pour déterminer si cette caractéristique est liée à des adaptations aux contraintes fonctionnelles exercées lors de la mastication ou à des activités para-masticatoires, ou bien si cela est dû à des processus évolutifs indépendants.

1. Introduction

The locality of Tighenif (formerly Ternifine) is situated in northwestern Algeria, in the province of Mascara. The site, a sand quarry near the village of Palikao, was discovered in 1870. Between 1954 and 1956, Arambourg(1954, 1955, 1957; Arambourg and Hoffstetter, 1954) carried out large-scale excavations that led to the discovery of human fossil remains associated with a lithic assemblage of Acheulean tools. The human fossil record consists of nine isolated teeth, two nearly complete adult mandibles (Tighenif 1 and 3), one adult hemi-mandible (Tighenif 2), and a parietal fragment (Tighenif 4). As a whole, the dental record suggests a minimum of five individuals, including four adults and one juvenile (Arambourg and Hoffstetter, 1963; Schwartz and Tattersall, 2003; Tillier, 1980). Based on biostratigraphy and paleomagnetic dating, the site was originally estimated to be c. 700 ka old (Geraads et al., 1986). However, a recent revision of the faunal list compared with those from East African sites suggests a late early Pleistocene age, close to 1 Ma as more likely (Geraads, 2016; Sahnouni and Van der Made, 2009). Accordingly, the fossil human assemblage from Tighenif would currently represent the earliest recovered so far from Northwest Africa, even if the region was certainly inhabited by humans since at least c. 2.4–1.9 Ma (Sahnouni et al., 2018).

The Tighenif human assemblage was originally attributed to *Atlanthropus mauritanicus* (Arambourg, 1954, 1955). However, because of some similarities with the Chinese dentognathic material from Zhoukoudian (Antón, 2003; Antón et al., 2007; Howell, 1960; Schwartz and Tattersall, 2003; Tillier, 1980), the assemblage was later integrated into the *Homo erectus* hypodigm. Based on archaeological and paleontological evidence, some authors have considered the possibility of relationships between the North African human groups represented at Tighenif and those peopling southern Europe at some points during the early–middle Pleistocene (Arribas and Palmqvist, 1999; Finlayson, 2002). However, while direct comparisons of the fossils from Tighenif with three late Early Pleistocene mandibles from the site of Gran Dolina-TD6, Spain, revealed a number of similarities, they have been interpreted as plesiomorphic for the genus *Homo* (Bermúdez de Castro et al., 1997, 2007, 2016). Given the particularly robust morphology of the Tighenif mandibles, Bermúdez de Castro et al. (2007) have suggested to consider these specimens as representatives of a *Homo ergaster* subspecies: *Homo ergaster mauritanicus*. More recently, the mandibles from Tighenif were compared with the Mauer specimen and found to be compatible with the *H. heidelbergensis* hypodigm, the latter being considered as an Afro-European species (Mounier, 2011; Mounier et al., 2009). However, the anterior symphyseal morphology of the Tighenif specimens as well as some Neanderthal-like features present in these specimens continue to raise some questions about their relationship with the anatomically modern humans and Neanderthal lineages (Mounier et al., 2009). Additionally, the microtomographic-based analysis of the inner structural organization of some deciduous and permanent teeth from the Algerian assemblage highlighted a complex pattern with a combination of unique, primitive, Neanderthal-like and modern human-like features (Macchiarelli et al., 2013; Zanolli and Mazurier, 2013; Zanolli et al., 2010). Thus, partly due to the robustness of the mandibles and to the rare comparative evidence available so far for human fossils sampling this chrono-geographical range, the taxonomic affinities of Tighenif specimens are still unclear.

Combined with the signal from the external morphology, the internal structure of the mandible potentially holds a blend of functional and taxonomic information useful in the study of the human fossil record (Daegling and Hotzman, 2003; Fiorenza et al., 2019; Grine and Daegling, 2017; Zanolli et al., 2017). A common assumption in biomechanical studies on craniofacial morphology is that there is a functional link between the mandibular structure and the forces triggered by mastication and other feeding behaviors (Daegling and Grine, 2006; Godinho et al., 2018; Holmes and Ruff, 2011; Hylander, 2006; Sella-Tunis et al., 2018; Toro-Ibacache et al., 2016). In fact, it is widely accepted that, under strain variations, the mandibular bone is remodeled in areas where it faces higher loads, i.e. where strain magnitude is above a particular threshold (Frost, 1987, 2003; Martinez-Maza et al., 2011; Pearson and Lieberman, 2004; Ruff et al., 2006; Schwartz-Dabney and Dechow, 2003). Thus, local variation in bone organization is, at least partly, linked with differences in functionally-related strain magnitude, and strain analysis can be employed to investigate whether cortical asymmetry is related to biomechanical demands (Fiorenza et al., 2019; Gröning et al., 2012; but see Ichim et al., 2006).

In the mandible, an asymmetric pattern of post-canine cortical bone thickness (CBT) distribution is documented in all anthropoids, where the lingual aspect of the corpus exhibits thinner cortical bone compared to the lateral aspect (Daegling, 1992; Daegling and Grine, 1991; Demes et al., 1984). This asymmetric pattern, which seems to transcend phylogenetic, allometric or ecological aspects, has been explained as resulting from the combined effects of vertical occlusal forces and torsions of the corpus during mastication (Daegling and Hotzman, 2003; Dechow and Hylander, 2000; Demes et al., 1984). This interpretation is

also supported by studies based on Finite Element Analysis (FEA) showing that high strain areas fit well with regions bearing higher CBT, thus highlighting a thicker buccal CBT in the posterior mandibular region (Gröning et al., 2012). However, the role and interpretation of this asymmetric mandibular CBT distribution is still debated. Ichim et al. (2006), for example, have suggested that the asymmetric pattern in modern human is not directly related to masticatory strains, i.e. strictly functionally-related, but rather the genetically-controlled result of a long-term modeling/remodeling balance process achieved during evolution. Asymmetry in cortical bone topography across the mandible could also reflect handedness, as it has been suggested for the Neanderthal specimen from Regourdou (Fiorenza et al., 2019; Volpato et al., 2012). With this respect, also the Algerian fossil specimen Tighenif 1 exhibits an asymmetric occlusal wear pattern of the post-canine dentition (Arambourg and Hoffstetter, 1963; Zanolli and Mazurier, 2013).

In the present study, we quantitatively assess the still unreported internal structural organization of the post-canine corpus of Tighenif 1 and Tighenif 2. Given the especially robust morphology of the two mandibles and their macrodont dentition (Arambourg, 1957; Bermúdez de Castro et al., 2007; Zanolli and Mazurier, 2013), we predict that these fossils will have an absolutely thicker cortical bone compared to extant humans. In addition, we also evaluate whether, and to what extent, buccal vs. lingual relative asymmetry in CBT distribution in the two fossils is affected by their robust morphology, i.e. if a larger size of the mandibular corpus tends to lower, or magnify, the pattern commonly measured in recent humans (Daegling and Hotzman, 2003; Demes et al., 1984).

2. Materials and methods

2.1. Materials

In the analyses, we uniquely considered the two specimens Tighenif 1 and Tighenif 2 because of the relatively poor preservation conditions of the partial mandible Tighenif 3, whose corpus is affected by numerous post-mortem breaks. To assess cortical bone post-canine distribution, we used X-ray microtomographic (μCT) records of the two Algerian fossil specimens performed in 2010 at the University of Poitiers using a X8050-16 Viscom AG equipment (microfocus directional X-ray source with an imaging system comprising a 9-inch triple-field intensifier coupled with a 12 bits, 1004 × 1004-pixel CCD). The parameters were as follows: voltage, 120 and 130 kV; current, 0.60 and 0.50 mA; a projection each 0.30° and 0.25°, respectively, for Tighenif 1 and Tighenif 2. The final volumes were reconstructed using the Feldkam algorithm with DigiCT v.2.3.3 (Digisens SA, France) in 8-bit format, with a final isotropic voxel size of 115.3 μm and 98.5 μm, respectively. The virtual reconstructions of these two specimens are represented in Fig. 1 A–B.

For comparison, we also used the mandibles of 10 (5 females and 5 males) adult modern humans (MH) selected from the Pretoria Bone Collection housed in the Department of Anatomy of the University of Pretoria, South Africa (L'Abbé et al., 2005). These materials were scanned at the microfocus X-ray tomography facility (MIXRAD) of the South African Nuclear Energy Corporation SOC Ltd (Necsa), Pelindaba, South Africa, using a Nikon XTH 225 ST (Metris). The parameters were as follows: voltage, 100 kV; current, 0.10 mA; a projection each 0.36°. Depending on their size, the final volumes of the 10 comparative specimens were reconstructed with an isotropic voxel size ranging from 66.5 μm to 79.6 μm. Ethical clearance for using this comparative sample was obtained from the Faculty of Health Sciences Research Ethics committee of the University of Pretoria (Ref. No. 340/2015).

3. Methods

A semi-automatic threshold-based segmentation of the virtual slices of all investigated specimens was preliminarily carried out using Avizo 8.1 (Visualization Science Group Inc) and ImageJ 1.51k (Schneider et al., 2012) following the half-maximum height methods (HMM; Spoor et al., 1993) and the region of interest thresholding methods (ROI-Tb protocol, Fajardo et al., 2002). In processing the record of the two fossil specimens Tighenif 1 and Tighenif 2, some manual corrections were locally necessary to virtually fill the cracks and reliably separate bone from matrix infill and air. On the Tighenif 1 mandible, major breaks are found on the left side, especially at the P3 level, at the inferior aspect of the mandible (Fig. 1C). This Algerian fossil was consolidated and reconstructed with plaster; however, the cortical and trabecular bone is still preserved and well-distinguished. The Tighenif 2 specimen presents local bone micro-breaks, but is better preserved than the one of Tighenif 1 (Fig. 1D). In fact, considering the estimated chronology of this material around 1 Ma, despite some cracks and larger fractures affecting the bone locally, the internal bony structure is well preserved. However, because of the variable positions of the fractures and local taphonomic alterations, a bi-dimensional analytical strategy was preferred to extract the maximum of information directly comparable between the two specimens.

We developed a specific protocol to estimate the CBT between the two premolars (P3/P4) and between the first and second molars (M1/M2) for both sides on each specimen. Firstly, a reference plane was defined as the plane fitting a set of semilandmarks along the most inferior line of the mandible corresponding to the inferior maximum of curvature of the (right or left) mandibular corpus (Fig. 2A). The posteriormost landmarks were placed distally to the M3. Then, CBT was assessed across four coronal slices manually oriented perpendicularly in the *XY* and *XZ* planes to the reference plane and to the alveolar arcade axis, respectively located between the P3 and P4 and between the M1 and M2 (Fig. 2B). We used tpsDig32 2.30 (Rohlf, 1997) to place semilandmarks on the four extracted slices of each specimen (two left and two right slices if available). We then defined a lingual and a buccal compartment on each slice: a line tangential to the alveolar margin has been drawn as the upper limit and the lingual and buccal compartments were created by drawing a second perpendicular line passing by

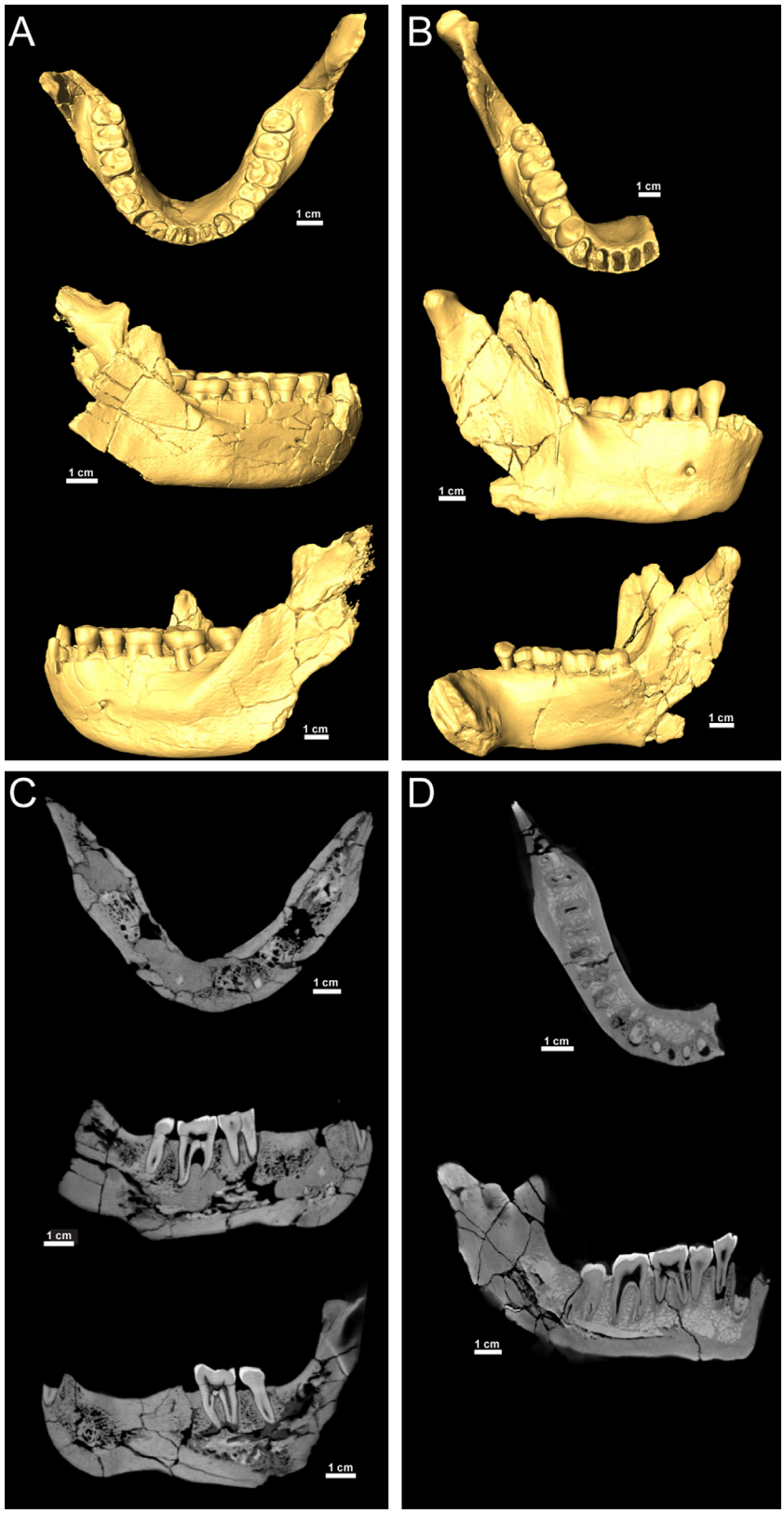

Fig. 1. Virtual renderings of the mandible Tighenif 1 (A) and of the hemi-mandible Tighenif 2 (B) in superior and lateral views. The longitudinal virtual cross-sections along the corpus of Tighenif 1 (C) and Tighenif 2 (D) illustrate the degree of preservation of the internal bone structure.

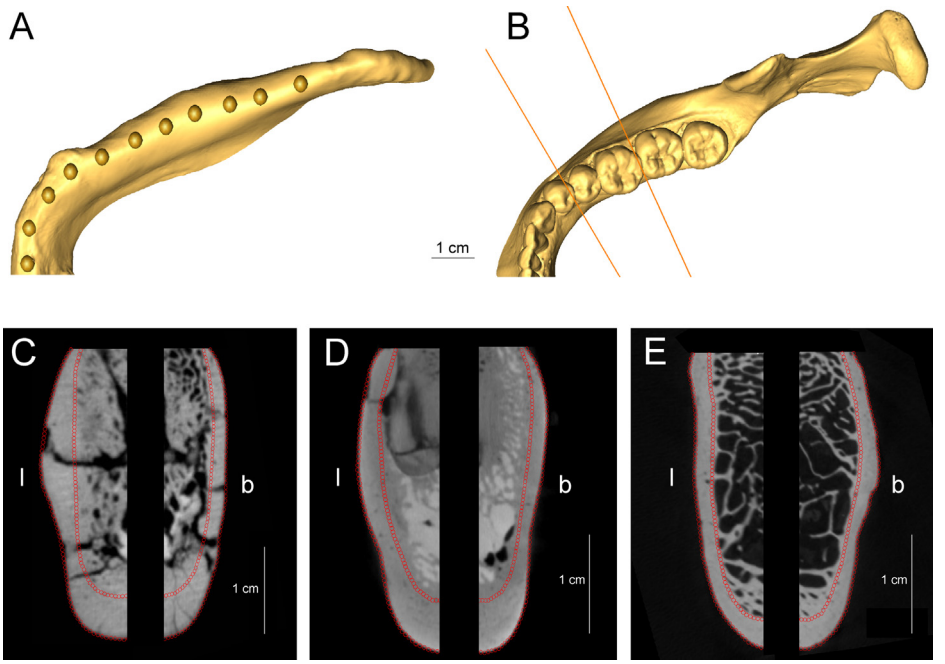

Fig. 2. Position of the semilandmarks on the inferior aspect of the mandible corpus used to fit a reference plane (A), and position of the slices perpendicular to the reference plane and to the mandibular corpus main axis (B), located between the P3 and P4 and M1 and M2. Virtual cross-sections set at the M1/M2 level in Tighenif 1 (C), Tighenif 2 (D) and a modern human (E) showing how the buccal (b) and lingual (l) aspects were delimited for their separate analyses, as well as the position of the semilandmarks placed along the external mandibular surface and on the internal cortical bone margin to assess the cortical bone thickness (CBT).

Fig. 2. Emplacement des points repères sur la partie inférieure de la mandibule utilisés pour positionner le plan de référence (A) et les positions des deux coupes perpendiculaires au plan de référence et à l'axe principal du corps mandibulaire, placées entre la P3 et la P4 ainsi qu'entre la M1 et la M2. Coupes virtuelles au niveau M1/M2 chez Tighenif 1 (C), Tighenif 2 (D) et un humain moderne (E), montrant comment l'aspect buccal (b) et l'aspect lingual (l) ont été délimités pour leur analyse séparée, ainsi que les points repères placés au niveau de la marge externe et interne de l'os cortical, utilisés pour mesurer l'épaisseur de l'os cortical (CBT).

the middle of the corpus until the most inferior point. Thereafter, a first curve was drawn following the external margins of the cortical bone, while a second one was placed along the periosteal cortical bone margins (Fig. 2C–E). An identical number of points for both curves was placed internally for each specimen in order to measure the cortical thickness as the shortest distance between the corresponding external and internal points. These curve points have been transformed into landmark coordinates by multiplying them by the voxel size. Then, a distance matrix was created for each specimen, calculating the distance between each pair of corresponding landmarks. The cortical area (CA, in mm^2) has also been measured on the buccal and lingual compartments with the Avizo 8.1 software.

Cortical bone thickness variation was analyzed on the sections taken along the mandible corpus in the statistical environment R 3.5.3 (R Core Team, 2019). Data were visualized using the package ggplot2 2.2.1 (Wickman, 2016). In order to allow direct comparisons between the fossil specimens and the extant human sample, we calculated a scale-free bi-dimensional Relative Cortical Thickness (2D RCT) index following the same analytical protocol used in Cazenave et al. (2017) for the distal humeral diaphysis. This parameter assesses the amount of cortical bone with respect to the volume occupied by the trabecular one. The RCT index is calculated as the Average Cortical Thickness (2D ACT) multiplied by 100 and divided by the square root of the trabecular area (TBA, in mm^2) ($2D\ RCT = 2D\ ACT \times 100/TBA^{1/2}$), where 2D ACT is the ratio between cortical area (CA, in mm^2) and the endosteal contour length (ecl, in mm) (2D ACT = CA/ecl, in mm). The 2D RCT calculation was distinctly performed for each lingual and buccal side. The percentages of asymmetry between the P3/P4 and M1/M2 sections, and between the lingual and buccal aspects were calculated on each corpus section with the formula found in Corruccini et al. (2005; buccal-lingual)/((buccal + lingual)/2). For all variables, a number of intra- and inter-observer tests for accuracy run by two independent observers revealed differences less or equal to 5% (e.g., Fiorenza et al., 2019).

Fig. 1. Rendus virtuels de la mandibule Tighenif 1 (A) et de l'hémi-mandibule Tighenif 2 (B) en vues supérieure et latérale. Les coupes virtuelles longitudinales passant au niveau du corpus des spécimens Tighenif 1 (C) et Tighenif 2 (D) permettent d'apprécier le degré de préservation de la structure osseuse interne.

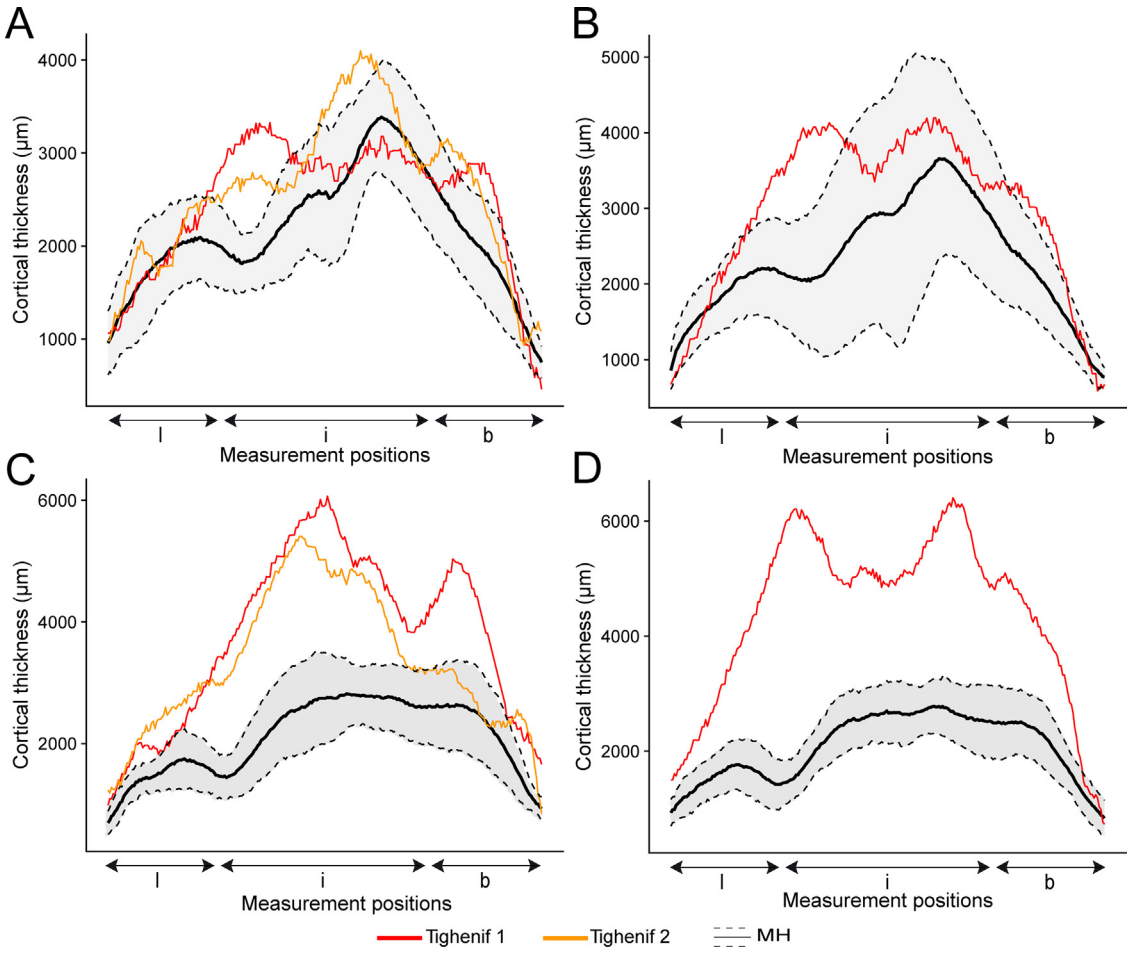

Fig. 3. Variations of CBT (in µm) at P3/P4 and M1/M2 from lingual (l) toward the inferior aspect (i) and to the buccal side (b) in the two Tighenif specimens and in ten modern humans (MH). The average value (dark line) and the variation expressed by plus or minus one standard deviation (grey area) are illustrated for the modern humans. A. Between the P3/P4 on the left side. B. Between the P3/P4 on the right side. C. Between the M1/M2 on the left side. D. Between the M1/M2 on the right side.

Fig. 3. Variations de CBT (en µm) entre P3/P4 et M1/M2 le long de l'aspect lingual (l) jusqu'à la partie inférieure (i) et en remontant vers l'aspect buccal (b) chez les deux fossiles de Tighenif et chez dix humains modernes (MH). La moyenne (ligne noire) ainsi que les variations (aire grise) représentées par plus ou moins un écart-type, sont illustrées pour notre échantillon de référence. A. Entre P3/P4 du côté gauche. B. Entre P3/P4 du côté droit. C. Entre M1/M2 du côté gauche. D. Entre M1/M2 du côté droit.

4. Results

Comparative cortical bone distribution on each bucco-lingual virtual section (respectively at the P3/P4 and M1/M2 levels on right and left parts the mandible corpus; see Fig. 2) was assessed in the two Tighenif specimens (only on the preserved left corpus for Tighenif 2) and extant human sample (Fig. 3A–D).

At the P3/P4 position (Fig. 3A–B), Tighenif 1, Tighenif 2 and extant humans exhibit a similar pattern on the left and right sides. More specifically, the two Algerian specimens mostly fall into the modern human (MH) range, which presents a high variability (meaning that some of MH specimens approximate the Tighenif cortical bone topography at this position). However, there are some exceptions, indeed, Tighenif 1 exceeds the MH range at the infero-lingual aspect on both side and Tighenif 2 displays higher cortical bone than Tighenif 1 and MH at the inferior aspect. By looking at the cortical area (CA, Table 1), the Tighenif specimens present higher CA than MH. While at the P3/P4 buccal level, Tighenif 2 has substantially higher values than Tighenif 1, the opposite condition is observed lingually. When considering the scale-free bi-dimensional Relative Cortical Thickness index (2D RCT; Table 2) at each P3/P4 section, the two Tighenif specimens display higher values than the average modern human condition. Tighenif 1 2D RCT exceeds that of Tighenif 2, showing its maximal value on the right side. With the CA and 2D RCT measurements, we can also observe different bucco-lingual asymmetry patterns between our specimens (Tables 1 and 3). The Tighenif specimens show a thicker buccal cortical bone, except at the left P3/P4 section for Tighenif 1. Modern humans exhibit the opposite pattern at this position, with a cortical bone thicker lingually than buccally for both right and left sides of the mandible.

Table 1
Cortical area (CA, in mm^2) assessed at the P3/P4 and M1/M2 levels, on the buccal and the lingual aspects, in the two Tighenif specimens and in a selected modern human (MH) sample ($n = 10$). The buccal-to-lingual difference asymmetry was assessed between the sections for each side.
Tableau 1
Aire de l'os cortical mesurée aux niveaux buccal et lingual des P3/P4 et M1/M2 chez les deux spécimens de Tighenif et dans notre échantillon humain (MH) actuel sélectionné ($n = 10$). Le pourcentage de différence a été évalué entre les sections de chaque côté.

	CA (mm^2)			
	Tighenif 1	Tighenif 2	MH	MH range
L				
P3/P4 buccal	85.5	111.6	42.7	22.3–58.2
P3/P4 lingual	91.0	85.1	54.8	28.8–88.2
M1/M2 buccal	112.7	86.0	49.4	22.0–79.3
M1/M2 lingual	101.9	81.9	44.8	26.1–72.0
R				
P3/P4 buccal	115.3		44.8	17.9–71.5
P3/P4 lingual	131.0		59.2	37.5–93.8
M1/M2 buccal	114.1		44.4	19.4–72.8
M1/M2 lingual	111.5		44.9	37.5–93.8
Asymmetry[a]				
P3/P4 left	−6.0%	27.0%	−25.0%	
M1/M2 left	10.0%	5.0%	10.0%	
P3/P4 right	−3.0%		−28.0	
M1/M2 right	2.0%		−1.0%	

[a] Asymmetry percentage assessed with the formula (buccal – lingual)/((buccal – lingual)/2) (Corruccini et al., 2005).

Table 2
2D Relative Cortical Thickness (2D RCT) assessed at the P3/P4 and M1/M2 positions in the two Tighenif specimens and in a modern human (MH) sample ($n = 10$).
Tableau 2
Épaisseur relative corticale 2D (2D RCT) mesurée au niveau des P3/P4 et M1/M2 chez les deux spécimens de Tighenif et dans l'échantillon humain (MH) actuel ($n = 10$).

	2D RCT			
	Tighenif 1	Tighenif 2	MH mean	MH range
L				
P3/P4	12.8	17.4	12.3	9.4–15.5
M1/M2	16.4	17.3	12.5	9.7–18.0
R				
P3/P4	19.7		12.2	9.4–15.5
M1/M2	15.1		12.0	9.7–18.0

Table 3
Buccal-to-lingual difference percentage of the 2D Relative Cortical Thickness (2D RCT) assessed between the P3/P4 and M1/M2 sections for each side in the two Tighenif specimens and in a modern human (MH) sample ($n = 10$).
Tableau 3
Pourcentage de différence entre l'épaisseur relative corticale 2D (2D RCT) buccale et linguale, évalué entre les sections P3/P4 et M1/M2 pour chaque côté chez les deux spécimens de Tighenif et dans l'échantillon humain (MH) actuel ($n = 10$).

	Asymmetry buccal vs. lingual[a]		
	Tighenif 1 (%)	Tighenif 2 (%)	MH mean (%)
L			
P3/P4	−23.0	17.0	−24.0
M1/M2	8.0	5.0	12.0
R			
P3/P4	6.0		−24.0
M1/M2	5.0		−1.0

[a] Asymmetry percentage assessed with the formula (buccal – lingual)/((buccal – lingual)/2) (Corruccini et al., 2005).

At the M1/M2 position, the Tighenif specimens present a similar cortical bone distribution, with a substantially thicker cortical bone than MH (reaching up to nearly three times the average modern human values), except for the left buccal aspect of Tighenif 2, which falls within the modern human range (Fig. 3C–D). Moreover, at the right M1/M2, the Tighenif 1 specimen presents a symmetrical bucco-lingual distribution that differs from that of the right side. The Algerian specimens also exhibit a higher CA compared to the MH range. Tighenif 1 systematically displays substantially higher values than Tighenif 2 for the left side (Table 1). When standardizing through the 2D RCT index (Table 2), the fossils from Tighenif still have a relatively thicker cortical bone than MH, and Tighenif 2 shows a thicker cortical bone than Tighenif 1. The Tighenif specimens display an absolutely and relatively thicker buccal compartment than the lingual one at the M1/M2 level (Tables 1 and 3). Our limited modern human sample shows more variation, with on average a thicker buccal cortical bone on the left side of the mandible, but equivalent values between the buccal and lingual compartments on the right side.

When comparing the P3/P4 and M1/M2 sections, the two fossil specimens exhibit different conditions. Tighenif 1 shows higher CA at the left molar level, while the contrary is observed for Tighenif 2. In addition, the right side Tighenif 1 also shows the opposite condition, with higher CA at the premolar level (Table 1). In modern humans, there is more variation, especially on the buccal aspect, but the lingual CA is on average higher at the premolar level than posteriorly. However, the Tighenif 1 mandible presents thicker cortical bone at the left M1/M2 section than at the left P3/P4 section and the opposite pattern on the right side, whereas Tighenif 2 and MH exhibit equivalent 2D RCT between the two positions (Table 2). The two fossil specimens show higher asymmetry at the left premolar level than posteriorly. The right side of Tighenif 1 displays similar levels of slight buccal asymmetry at both premolar and molar levels. In modern humans, the left and right P3/P4 sections show similarly high magnitudes of asymmetry, comparable to those of the left side of both specimens from Tighenif, but a lower degree of asymmetry at the M1/M2 level.

5. Discussion and conclusions

In this study, we aimed to characterize the post-canine cortical bone thickness (CBT) in the Tighenif 1 and Tighenif 2 mandibular remains. Our results showed that both specimens have comparable absolute and relative CBT and distribution patterns at the P3/P4 and M1/M2 levels. In Tighenif 1, in which both sides of the mandible are preserved, there is a relationship between the relative thick cortical bone at the right P3/P4 level and the important dental occlusal wear found on this side (Arambourg and Hoffstetter, 1963; Zanolli and Mazurier, 2013). This may suggest that the cortical bone topography of this specimen could be biomechanically related to masticatory and/or paramasticatory differential loadings (Daegling and Hotzman, 2003; Fiorenza et al., 2019; Gröning et al., 2012). Recently, Fiorenza et al. (2019) have also found a concordance between wear asymmetry and thicker cortical bone

distribution in the Neanderthal specimen Regourdou 1, likely in relation to the right-handedness and paramasticatory activities previously reported for this individual (Volpato et al., 2012).

There is also a noticeable difference in maximal CBT and distribution pattern on the left buccal side of Tighenif 1 compared with that of Tighenif 2. This localized difference could be due to inter-individual variation (including sexual dimorphism), possibly linked to some subtle expression of the mandibular torus (Arambourg and Hoffstetter, 1963). In addition, it is noteworthy that Tighenif 2 has a CBT mostly equivalent to that of Tighenif 1, but shows less advanced dental occlusal wear (Arambourg and Hoffstetter, 1963; Zanolli and Mazurier, 2013). Thus, it would be too simple to consider that the differences in CBT distributions and the very thick cortical bone in the Tighenif specimens were only explained by a functional response during the masticatory process. It is also important to note that the smaller and less robust specimen Tighenif 2 has been suggested to represent a younger individual than Tighenif 1 and/or could also be a female (Arambourg and Hoffstetter, 1963).

We also highlighted major differences along the post-canine corpus between the two Tighenif specimens and modern humans. Tighenif CBT absolute values and topographic distribution approximate the modern condition at the P3/P4 level (especially on the left side) while they substantially deviate from the modern human pattern posteriorly. In terms of relative values, the 2D RCT index supports the proportionally more robust state of the Tighenif specimens compared with modern humans.

Biomechanical studies of extant human mandibles also suggested that the torsional moments related to masticatory constraints are greatly reduced in the anterior corpus (Hylander, 1984), while lateral transverse bending or “wishboning” stresses increase posteriorly particularly along the lingual margins (Daegling and Hotzman, 2003; Dechow and Hylander, 2000; Demes et al., 1984). The Tighenif mandibles show differences in buccal vs. lingual CBT. Ichim et al. (2006) have suggested that, in modern humans, this asymmetric pattern between buccal and lingual aspects is not related to masticatory strains. Instead, it could result from a retained evolutionary process possibly linked with the reduction of the face and tooth size in *H. sapiens*. In any case, the role and interpretation of this asymmetric mandibular CBT distribution is debated and, as shown in our limited comparative sample, there seems to be some variation that should be investigated further. The two Tighenif specimens exhibit thicker buccal than lingual cortical bone at the post-canine level (except for a single spot at the left P3/P4 section, where the bone is locally fractured and thus may affect the CBT assessment). This condition resembles what has been described for the modern human condition (Daegling and Hotzman, 2003; Dechow and Hylander, 2000; Demes et al., 1984). Martinez-Maza et al. (2011) have also suggested that the buccal side of the mandibular ramus in Neanderthals is affected by higher remodeling activities resulting from mechanical force. This was also evidenced in the Neanderthal specimen Regourdou 1 where the cortical bone under the P3 exhibits an asymmetric pattern in CBT distribution with the left buccal aspect being thicker (Fiorenza et al., 2019).

Substantial size and morphological differences between the fossil specimens from Tighenif and modern human mandibles represent taxonomic features likely reflecting adaptations to withstand biomechanical stresses in relation to the facial architecture (Ledogar et al., 2017; Strait et al., 2010). Such differences could be explained by dissimilarities in physiology. Indeed, numerous hormones are implicated in the systemic control of bone modeling (reshaping of bone through modeling drifts that occur primarily during growth), and remodeling (replacement of old or damaged bone tissue through a process of coupled resorption and formation) (Hublin, 1978, 1986; Kini and Nandeesh, 2012; Raggatt and Partridge, 2010 have argued that many morphological features of *H. erectus*, including cranial superstructures, thick cranial bones, and thick post-cranial cortical bone, could be the result of a single physiological process as a variation in endocrine production). While this may result from an allometric and differential bone growth related to the increase in size and robusticity, it is still unclear whether it could be of adaptive value.

The robusticity of the two Tighenif specimens is associated with the strong development of superstructures such as the sulcus intertoralis, lateral prominence, and the wide extramolar sulcus. In addition, the lateral prominence is positioned between the P3/P4 for Tighenif 1, between the M1/M2 for Tighenif 2 and the mental foramen is found between the P3/P4 for these two African specimens. Moreover, all the premolars from the Tighenif 1 and Tighenif 2 specimens exhibit complex 2R Tomes’ root morphologies (Prado-Simón et al., 2012a, 2012b; Zanolli and Mazurier, 2013). Altogether, these morphological differences may have an impact on the CBT assessment, but are also part of the variation characteristic of a taxon. To this date, only a few studies have characterized the internal structure of the mandibular corpus in fossil hominins (Daegling and Grine, 1991; Fiorenza et al., 2019; Zanolli et al., 2017), while the extent of variation of the modern human condition remains to be investigated. Pending future comparisons of the internal bony signature of the Tighenif mandibles with other fossil specimens and larger modern human samples, considering the already proposed mix of features, including the expression of Neanderthal-like features on the external bone morphology and teeth (Mounier et al., 2009; Zanolli et al., 2010; Zanolli and Mazurier, 2013), we hypothesize that the CBT condition in the Tighenif mandible specimens may approximate the Neanderthal pattern, notably at the molar level.

Acknowledgements

The microCT record of Tighenif 1 and Tighenif 2 has been realized and made available by R. Macchiarelli and A.M. thanks to the collaboration provided at the MNHN Paris by C. Argot and H. Lelièvre. For access to the modern human comparative material and for scanning, we acknowledge F. de Beer, J. Hoffman, G.C. Kruger, A.C. Oettlé. For scientific discussion and methodological support, we are grateful to S. Cobb, P. Cox, L. Fitton, R. Macchiarelli and P. O’Higgins. Research supported by the French INEE–CNRS and the AMI grant of the University of Toulouse. C.E.G.T. was supported

by the University of Pretoria Postgraduate Research Support Bursary.

References

Antón, S.C., 2003. Natural history of *Homo erectus*. Yearb. Phys. Anthropol. 46, 126–170.

Antón, S.C., Spoor, F., Fellmann, C.D., Swisher III., C.C., 2007. Defining *Homo erectus*: size considered. In: Henke, W., Tattersall, I. (Eds.), Handbook of Paleoanthropology. Springer, New York, pp. 1655–1695.

Arambourg, C., 1954. L'hominine fossile de Ternifine (Algérie). C. r. hebd. seances Acad. sci. 239, 893–895.

Arambourg, C., 1955. A recent discovery in human paleontology: *Atlanthropus* of Ternifine (Algeria). Am. J. Phys. Anthropol. 13, 191–201.

Arambourg, C., 1957. Récentes découvertes de paléontologie humaine réalisées en Afrique du Nord française (L'*Atlanthropus* de Ternifine – L'Hominien de Casablanca). In: Clarck, J.D., Cole, S. (Eds.), Proceedings of the Third Panafrican Congress on Prehistory. Chatto and Windus, London, pp. 186–194.

Arambourg, C., Hoffstetter, R., 1954. Découverte en Afrique du Nord des restes humains du Paléolithique inférieur. C. r. hebd. seances Acad. sci. 239, 72–74.

Arambourg, C., Hoffstetter, R., 1963. Le gisement de Ternifine. Arch. Inst. Paleontol. Hum. 32, 1–190.

Arribas, A., Palmqvist, P., 1999. On the ecological connection between sabre-tooths and hominids: faunal dispersal events in the lower Pleistocene and a review of the evidence for the first human arrival in Europe. J. Archeol. Sci. 26, 571–585.

Bermúdez de Castro, J.M., Arsuaga, J.L., Carbonell, E., Rosas, A., Maztínez, I., Mosquera, M., 1997. A Hominid from the lower Pleistocene of Atapuerca, Spain: possible ancestor to Neandertals and modern humans. Science 276, 1392–1395.

Bermúdez de Castro, J.M., Martinón-Torres, M., Gómez-Robles, A., Prado, L., Sarmiento, S., 2007. Comparative analysis of the Gran Dolina-TD6 (Spain) and Tighennif (Algeria) hominin mandibles. Bull. Mem. Soc. Anthropol. Paris 19, 149–167.

Bermúdez de Castro, J.M., Martinón-Torres, M., Rosell, J., Blasco, R., Arsuaga, J.L., Carbonell, E., 2016. Continuity *versus* discontinuity of the human settlement of Europe between the late early Pleistocene and the early middle Pleistocene. The mandibular evidence. Quat. Sci. Rev. 153, 51–62.

Cazenave, M., Braga, J., Oettlé, A., Thackeray, J.F., Beer, F., Hoffman, J., Endalamaw, M., Redea, B.E., Puymerail, L., Macchiarelli, R., 2017. Inner structural organization of the distal humerus in *Paranthropus* and *Homo*. C. R. Palevol 16, 521–532.

Corruccini, R.S., Townsend, G.C., Schwerdt, W., 2005. Correspondence between enamel hypoplasia and ondontometric bilateral asymmetry in Australian twins. Am. J. Phys. Anthropol. 126, 177–182.

Daegling, D.J., 1992. Mandibular morphology and diet in the genus *Cebus*. Int. J. Primatol. 13, 545–570.

Daegling, D.J., Grine, F.E., 1991. Compact bone distribution and biomechanics of early hominid mandibles. Am. J. Phys. Anthropol. 86, 321–339.

Daegling, D.J., Grine, F.E., 2006. Mandibular biomechanics and the paleontological evidence for the evolution of human. In: Ungar, P.S. (Ed.), Evolution of the Human Diet: The Know, The Unknown, and the Unknowable. Oxford University Press, New York, pp. 77–105.

Daegling, D.J., Hotzman, J.L., 2003. Functional significance of cortical bone distribution in anthropoid mandibles: an in vitro assessment of bone strain under combined loads. Am. J. Phys. Anthropol. 122, 38–50.

Dechow, P.C., Hylander, W.L., 2000. Elastic properties and masticatory bone stress in the macaque mandible. Am. J. Phys. Anthropol. 112, 557–571.

Demes, B., Preuschoft, H., Wolff, J.E.A., 1984. Stress-strength relationships in the mandibles of hominoids. In: Chivers, D.J., Wood, B.A., Bilsborough, A. (Eds.), Food Acquisition and Processing in Primates. Plenum Press, London, pp. 369–390.

Fajardo, R.J., Ryan, T.M., Kappelman, J., 2002. Assessing the accuracy of high-resolution X-ray computed tomography of primate trabecular bone by comparisons with histological sections. Am. J. Phys. Anthropol. 118, 1–10.

Finlayson, C., 2002. The role of climate in the spatio-temporal pattern of human colonization and extinction in the Pleistocene with specific reference to the Mediterranean Region. In: Ruiz-Zapara, B., et al. (Eds.), Quaternary Climatic Changes and Environmental Crises in the Mediterranean Regions. Universidad de Alcala de Henares, Madrid, pp. 1–8.

Fiorenza, L., Benazzi, S., Kullmer, O., Mazurier, A., Zanolli, C., Macchiarelli, R., 2019. Dental macrowear and cortical bone distribution of the Neanderthal mandible from Regourdou (Dordogne, southwestern France). J. Hum. Evol. 132, 174–188.

Frost, H.M., 1987. Bone "mass" and the "mechanostat": a proposal. Anat. Rec. 219, 1–9.

Frost, H.M., 2003. Bone's mechanostat: a 2003 update. Anat. Rec. 275A, 1081–1101.

Geraads, D., 2016. Pleistocene Carnivora (Mammalia) from Tighenif, Algeria. Gebios 49, 445–458.

Geraads, D., Hublin, J.J., Jaeger, J.J., 1986. The Pleistocene hominid site of Ternifine Algeria: new results on the environment, age, and human industries. Quat. Res. 25, 380–386.

Godinho, R.M., Fitton, L.C., Toro-Ibacache, V., Stringer, C.B., Lacruz, R.S., Bromage, T.G., O'Higgins, P., 2018. The bitting performance of *Homo sapiens* and *Homo heidelbergensis*. J. Hum. Evol. 118, 56–71.

Grine, F.E., Daegling, D.J., 2017. Functional morphology, biomechanics and the retrodiction of early hominin diets. C. R. Palevol 16, 613–631.

Gröning, F., Fagan, M., O'Higgins, P., 2012. Comparing the distribution of strains with the distribution of bone tissue in a human mandible: a finite element study. Anat. Rec. 296, 9–18.

Holmes, M.A., Ruff, C.B., 2011. Dietary effects on development of the human mandibular corpus. Am. J. Phys. Anthropol. 145, 615–628.

Howell, F.C., 1960. European and Northwest African middle Pleistocene hominids. Curr. Anthropol. 1, 195–232.

Hublin, J.-J., (PhD dissertation), 1978. Le torus occipital transverse et les structures associées : évolution dans le genre *Homo*. Université Pierre-et-Marie-Curie, Paris-6, Paris.

Hublin, J.-J., 1986. Some comments on the diagnostic features of *Homo erectus*. Anthropos (Brno) 23, 175–187.

Hylander, W.L., 1984. Stress and strain in the mandibular symphysis of primates: a test of competing hypotheses. Am. J. Phys. Anthropol. 64, 1–46.

Hylander, W.L., 2006. Functional, Anatomy and Biomechanics of the Masticatory Apparatus. In: Temporomandibular Disorders and Evidenced Approach to Diagnosis and Treatment. Quintessence Publishing, New York, pp. 1–34.

Ichim, I., Kieser, J.A., Swain, M.V., 2006. Functional significance of strain distribution in the human mandible under masticatory load: numerical predictions. Arch. Or. Biol. 52, 465–473.

Kini, U., Nandeesh, B.N., 2012. Physiology of bone formation, remodeling and metabolism. In: Fogelman, I., Gnanasegaran, G., Van der Wall, H. (Eds.), Radionuclide and Hybrid Bone Imaging. Springer, Berlin, Heidelberg, pp. 29–57.

L'Abbé, E.N., Loots, M., Meiring, J.H., 2005. The Pretoria bone collection: a modern South African skeletal sample. Homo 56, 197–205.

Ledogar, J.A., Benazzi, S., Smith, A.L., Weber, G.W., Carlson, K.B., Dechow, P.C., Grosse, I.R., Ross, C.F., Richmond, B.G., Wright, B.W., Wang, Q., Byron, C., Carlson, K.J., De Ruiter, D.J., Pryor Mcintosh, L.C., Strait, D.S., 2017. The biomechanics of bony facial "buttresses" in South African australopiths: an experimental study using finite element analysis. Anat. Rec. 300, 171–195.

Macchiarelli, R., Bayle, P., Bondioli, L., Mazurier, A., Zanolli, C., 2013. From outer to inner structural morphology in dental anthropology. The integration of the third dimension in the visualization and quantitative analysis of fossil remains. In: Scott, G.R., Irish, J.D. (Eds.), Anthropological Perspectives on Tooth Morphology. Genetics, Evolution, Variation. Cambridge University Press, Cambridge, UK, pp.250–277.

Martinez-Maza, C., Rosas, A., García-Vargas, S., Estalrrich, A., de la Rasilla, M., 2011. Bone remodelling in Neanderthal mandibles from the El Sidrón site (Asturias, Spain). Biol. Lett. 7, 593–596.

Mounier, A., 2011. Définition du taxon *Homo heidelbergensis* Schoetensack, 1908 : analyse phénétique du massif facial supérieur des fossiles du genre *Homo* du Pléistocène moyen. Bull. Mem. Soc. Anthropol. Paris 23, 115–151.

Mounier, A., Marchal, F., Condemi, S., 2009. Is *Homo heidelbergensis* a distinct species? New insight on the Mauer mandible. J. Hum. Evol. 56, 219–246.

Pearson, O.M., Lieberman, D.E., 2004. The aging of Wolff's "law": ontogeny and responses to mechanical loading in cortical bone. Am. J. Phys. Anthropol. 125, 63–99.

Prado-Simón, L., Martinón-Torres, M., Baca, P., Gómez-Roblez, A., Lapresa, M., Carbonell, E., Bermúdez de Castro, J.M., 2012a. A morphological study on the tooth roots of the Sima del Enfante mandible (Atapuerca, Spain): a new classification of the teeth – biological and methodological considerations. Anthropol. Sci. 120, 61–72.

Prado-Simón, L., Martinón-Torres, M., Baca, P., Gómez-Roblez, A., Lapresa, M., Carbonell, E., Bermúdez de Castro, J.M., 2012b. Three-dimensional

evaluation of root canal morphology in lower second premolars of early and middle Pleistocene human populations from Atapuerca (Burgos, Spain). Am. J. Phys. Anthropol. 147, 452–461.
Raggatt, L.J., Partridge, N.C., 2010. Cellular and molecular mechanisms of bone remodeling. J. Biol. Chem. 285, 25103–25108.
R Core Team, 2019. R: A Language and Environment for Statistical Computing. R Foundation for Statistical Computing, Vienna, Austria (Available at: http://www.R-project.org/).
Rohlf, F.J., 1997. tpsDig: Digitize Landmarks and Outlines. Version 2. 29. Apr 4 (cited 23 Oct 2016. Available at: http://life.bio.sunysb.edu/morph/).
Ruff, C., Holt, B., Trinkaus, E., 2006. Who's afraid of the big bad Wolff?: "Wolff's law" and bone functional adaptation. Am. J. Phys. 126, 484–498.
Sahnouni, M., Parés, J.M., Duval, M., Cáceres, I., Harichane, Z., Van der Made, J., Pérez-González, A., Abdessadok, S., Kandi, N., Derradji, A., Medig, M., Boulaghraif, K., Semaw, S., 2018. 1.9-million- and 2.4-million-year-old artifacts and stone tool–cutmarked bones from Ain Boucherit, Algeria. Science 362, 1297–1301.
Sahnouni, M., Van der Made, J., 2009. The Oldowan in North Africa Within a Biochronological Framework. The Cutting Edge: New Approaches to the Archeology of Human Origins. Stone Age Institute Press, Bloomington, IN, USA, pp. 179–210.
Schneider, C.A., Rasband, W.S., Eliceiri, K.W., 2012. NIH Image to ImageJ: 25 years of image analysis. Nat. Methods 9, 671–675.
Schwartz, J.H., Tattersall, I., 2003. The Human Fossil Record. Craniodental Morphology of Genus *Homo* (Africa and Asia), vol. 2. Wiley-Liss, Hoboken, NJ, USA.
Schwartz-Dabney, C.A., Dechow, P.C., 2003. Variations in cortical material properties throughout the human dentate mandible. Am. J. Phys Anthropol. 120, 252–277.
Sella-Tunis, T., Pokhojaev, A., Sarig, R., O'Higgins, P., May, H., 2018. Human mandibular shape is associated with masticatory muscle force. Sci. Rep. 8, 6042.
Spoor, C.F., Zonneveld, F.W., Macho, G.A., 1993. Linear measurements of cortical bone and dental enamel by computed tomography: applications and problems. Am. J. Phys. Anthropol. 91, 469–484.
Strait, D.S., Grosse, I.R., Dechow, P.C., Smith, A.L., Wang, Q., Weber, G.W., Neubauer, S., Slice, D.E., Chalk, J., Richmond, B.G., Lucas, P.W., Spencer, M.A., Schrein, C., Wright, B.W., Byron, C., Ross, C.F., 2010. The structural rigidity of the cranium of *Australopithecus africanus*: implications for diet, dietary adaptations, and the allometry of feeding biomechanics. Anat. Rec. 293, 583–593.
Tillier, A.M., 1980. Les dents d'enfant de Ternifine (Pléistocène moyen d'Algérie). L'Anthropologie 84, 413–421.
Toro-Ibacache, V., Muñoz, V.Z., O'Higgins, P., 2016. The relationship between skull morphology, masticatory muscle force and cranial skeletal deformation during biting. Ann. Anatomy–Anat. Anz. 203, 59–68.
Volpato, V., Macchiarelli, R., Guatelli-Steinberg, D., Fiore, I., Bondioli, L., Frayer, D.W., 2012. Hand to mouth in a Neandertal: right-handedness in Regourdou 1. PLoS One 7, e43949.
Wickman, H., 2016. ggplot2: Elegant Graphics for Data Analysis. Springer-Verlag, New York (Available at: https://ggplot2.tidyverse.org).
Zanolli, C., Mazurier, A., 2013. Endostructural characterization of the *H. heidelbergensis* dental remains from the early middle Pleistocene site of Tighenif, Algeria. C. R. Palevol 12, 293–304.
Zanolli, C., Bayle, P., Macchiarelli, R., 2010. Tissue proportions and enamel thickness distribution in the early middle Pleistocene human deciduous molars from Tighenif, Algeria. C. R. Palevol 9, 341–348.
Zanolli, C., Dean, M.C., Assefa, Y., Bayle, P., Braga, J., Condemi, S., Endalamaw, M., Engda Redea, B., Macchiarelli, R., 2017. Structural organization and tooth development in a *Homo* aff. *erectus* juvenile mandible from the early Pleistocene site of Garba IV at Melka Kunture, Ethiopian highlands. Am. J. Phys. Anthropol. 162, 549–553.